

**NANOCOMPOSITE POLYMER ELECTROLYTES**

**F49620-98-1-0140**

***FINAL REPORT***

Emmanuel P. Giannelis  
Materials Science and Engineering  
Cornell University

Submitted to

Lt.Col. Paul C. Trulove, Ph. D.  
Program Manager, Surface and Interfacial Science  
AFOSR/NL

20010320 065

## REPORT DOCUMENTATION PAGE

AFRL-SR-BL-TR-01-

Public reporting burden for this collection of information is estimated to average 1 hour per response, including gathering and maintaining the data needed, and completing and reviewing the collection of information. Send collection of information, including suggestions for reducing this burden, to Washington Headquarters Service, Davis Highway, Suite 1204, Arlington, VA 22202-4302, and to the Office of Management and Budget, Paperwork Project, Washington, DC 20503.

ces,  
this  
rson

0753

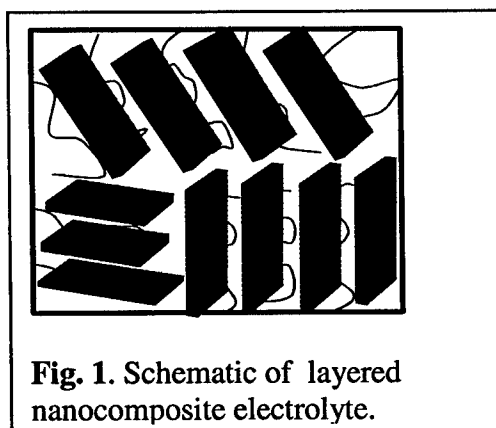
1. AGENCY USE ONLY (Leave blank)		2. REPORT DATE	3. REPORT TYPE AND DATES COVERED Final - 1 January 1998 - 30 November 2000	
4. TITLE AND SUBTITLE Nanocomposite Polymer Electrolytes			5. FUNDING NUMBERS F49620-98-1-0140	
6. AUTHOR(S) Dr. Emmanuel P. Giannelis Material Science and Engineering				
7. PERFORMING ORGANIZATION NAME(S) AND ADDRESS(ES) Cornell University Ithaca, NY 14853			8. PERFORMING ORGANIZATION REPORT NUMBER	
9. SPONSORING/MONITORING AGENCY NAME(S) AND ADDRESS(ES) AFOSR/NL 801 North Randolph Street, Room 732 Arlington, VA 22203-1977			10. SPONSORING/MONITORING AGENCY REPORT NUMBER	
11. SUPPLEMENTARY NOTES				
12a. DISTRIBUTION AVAILABILITY STATEMENT APPROVED FOR PUBLIC RELEASE: DISTRIBUTION UNLIMITED			AIR FORCE OFFICE OF SCIENTIFIC RESEARCH (AFOSR) NOTICE OF TRANSMITTAL DTIC. THIS TECHNICAL REPORT HAS BEEN REVIEWED AND IS APPROVED FOR PUBLIC RELEASE LAW AFR 180-12. DISTRIBUTION IS UNLIMITED.	
13. ABSTRACT (Maximum 200 words) Using Monte Carlo, MC, and Molecular Dynamics, MD, computer simulations we have shown that the polymer chains at the interface organize into discrete layers parallel to the crystalline inorganic surface. In spite of this ordering, the polymer chains retain a disordered, liquid-like structure consistent with our small angle neutron scattering, SANS, experiments.				
14. SUBJECT TERMS			15. NUMBER OF PAGES 20	
			16. PRICE CODE	
17. SECURITY CLASSIFICATION OF REPORT Unclass	18. SECURITY CLASSIFICATION OF THIS PAGE Unclass	19. SECURITY CLASSIFICATION OF ABSTRACT Unclass	20. LIMITATION OF ABSTRACT	

## Objectives

Solid-state, high-density, rechargeable batteries are key to the development of several military and commercial applications, from portable electronics to electric vehicles to back-up power sources in aircraft. The objective of this program is to develop and evaluate a new generation of nanocomposite electrolytes for future military and commercial applications.

One interesting class of nanocomposite electrolytes is made by intercalating polymers such as PEO between the individual layers of a layered host such as a layered silicate (Fig. 1). The resulting materials combine relatively high ambient conductivity with single ion conduction characteristics. (Note that in these nanocomposite electrolytes, 1 nm thick, negatively-charged silicate layers are separated by interlayers, which contain charge-compensating Li-cations and polymer chains. Because of their massive lateral dimensions, the silicate anions are immobile.)

Due to the structural regularity of the inorganic host, *the nanocomposites are excellent model systems to probe and understand the structure and dynamics at the interface and relate these molecular features to macroscopic properties such as ionic conductivity.* By combining computer simulations with experiments a detailed picture of the structure and mobility of the polymer and the ions at the interface has started to emerge. Below we summarize our recent results on nanocomposite electrolytes.



## Accomplishments/New Findings

Using Monte Carlo, MC, and Molecular Dynamics, MD, computer simulations we have shown that the polymer chains at the interface organize into discrete layers parallel to the crystalline inorganic surface (Fig. 2,3). In spite of this ordering, the polymer chains retain a disordered, liquid-like structure consistent with our small angle neutron scattering, SANS, experiments.



**Fig. 2.** Snapshot of dry (top) and solvated (bottom) PEO-Li-silicate nanocomposites. The silicate crystals are shown as polyhedra,  $\text{Li}^+$  as blue spheres, PEO as the grey and red spheres and solvent as the green sticks.

In the absence of a solvent the cations are basically pinned to the inorganic surface rather than being coordinated with PEO. In the solvated nanocomposites, some cations still reside near the surface but a large number of the Li cations have now moved away from the surface. The cations coordinate primarily to the solvent molecules or the surface but not to the polymer chains. In addition, MD simulations show that solvated Li ions are much more mobile than those pinned to the surface.

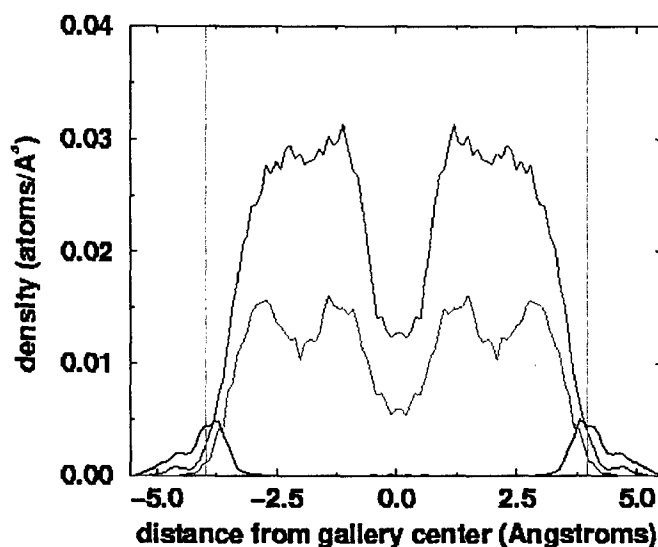


**Fig. 3.** Density profile for PEO-Li-silicate nanocomposite: black line cation, green line PEO oxygen and red line PEO carbon. The vertical gray lines represent the outer edges of the silicate oxygen surface.

Our tools for dynamics include NMR and dielectric relaxation spectroscopy. Using surface-sensitive cross polarization with spin-echo experiments in collaboration with D. Zax from Chemistry we showed that the polymer chains at the interface exhibit a wide range of relaxation times. On one hand, some polymer segments at the interface are more mobile (i.e. more *liquid-like*) than the bulk polymer at the same temperature. On the other hand, the interface polymer appears to exhibit *solid-like* character even at temperatures well above the bulk  $T_g$ . Similar behavior was observed using dielectric

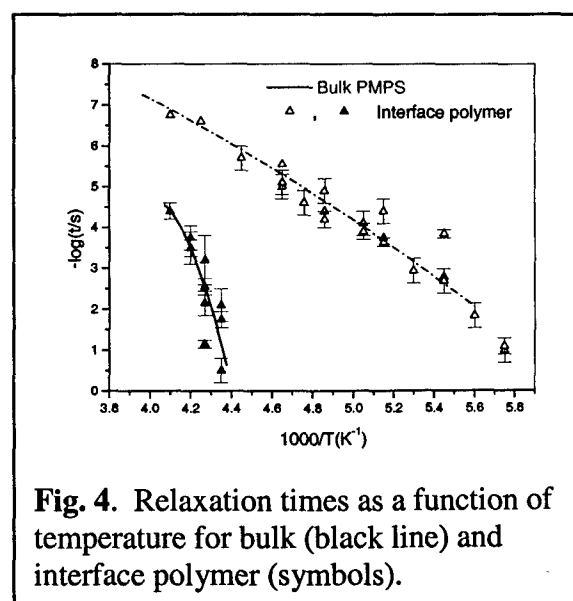


**Fig. 4.** Relaxation times as a function of temperature for bulk (black line) and interface polymer (symbols).

spectroscopy. The polymer at the interface exhibits two relaxation modes. The new mode is much faster than the bulk-polymer  $\alpha$  relaxation, with much weaker temperature dependence.

Intuitively, one might have expected the polymer at the interface to be less mobile compared to the bulk polymer, as "confinement" of the polymer chains within a few nanometers should increase their solid-like character and decrease their mobility. In fact, a decrease in mobility of polymers near the interface has been suggested to account for the presence of two glass transitions (the second at a higher temperature) in polymer composites.

The results on polymer dynamics in the nanocomposites can be rationalized using the computer simulations discussed above. As the polymer organizes into discrete layers, areas of high and low density coexist in close proximity to each other. The wide range of relaxation times found experimentally reflects the density variation as segments of low and high density would exhibit fast and slow dynamics, respectively. The absence of crystallization and the liquid-like character of the interface polymer definitely support the enhanced ionic conductivity observed in the nanocomposites.

More technical details on our work are given in the attached publications.

#### **Personnel Supported**

Emmanuel P. Giannelis – PI

Emily Hackett - graduate student

M. Jacob - postdoctoral associate

#### **Publications**

E.P. Giannelis, R. Krishnamoorti and E. Manias, "Polymer-Silicate Nanocomposites: Model Systems for Confined Polymers and Polymer Brushes", in Advances in Polymer Science, S. Granick, Ed., Springer, **138**, **1999**.

D.B. Zax, D.-K. Yang, P.A. Santos, H. Hegemann, E.P. Giannelis and E. Manias, "Dynamical Heterogeneity in Nanoconfined Poly(styrene) Chains", Journal of Chemical Physics, **112**, 2945, **2000**.

E. Manias, A.Z. Panagiotopoulos, D.B. Zax and E.P. Giannelis, "Structure and Dynamics of Nanocomposite Polymer Electrolytes", CMS Workshop Lectures, The Clay Minerals Society, **vol. 13**, **2000**.

E. Hackett, E. Manias and E.P. Giannelis, "Computer Simulation Studies of PEO/Layer Silicate Nanocomposites", Chemistry of Materials, **12**, 2161, **2000**.

J. Bujdák, E. Hackett and E.P. Giannelis, "Nanocomposite Polymer Electrolytes: Effect of Layer Charge on the Intercalation of Polyethylene Oxide in Layered Silicates", Chemistry of Materials, **12**, 2168, **2000**.

R.A. Vaia and E.P. Giannelis, "Polymer Nanocomposites: Status and Opportunities", MRS Bulletin, submitted.

E.P. Giannelis, "Polymer-Layer Silicate Nanocomposites: An Overview", Journal of American Ceramic Society, submitted.

G. Ji, F. Clement and E.P. Giannelis, "Nanofiller Modification of Phase Stability in PS/PMMA Blends", MRS Proceedings, R.P. Hjelm, A.I. Nakatani, M. Gerspacher and R. Krishnamoorti, Eds., submitted.

L.G. Scanlon, W.T. Krawiec and E.P. Giannelis, "Ion Conducting Electrolyte Material Containing a Lithium Porphyrin Complex", U.S Patent, 6,010,805, **2000**.

### **Interactions/Transitions**

The PI is frequently invited to present our work in nanocomposites at various meetings/conferences. Here is a sampling of invited talks for 2000.

#### *Invited Seminars to Conferences/Universities/National Labs*

115. Engineering Conference on Nanostructured Materials, Maui, HA (January 2000)
116. 14<sup>th</sup> Annual CFMR Symposium, E. Lansing, MI (February 2000)
117. Additives 2000, Clearwater Beach, FL (April 2000)
118. Commercialization of Nanostructured Materials, Miami, FL (April 2000)
119. MSI Consortium Conference, Key West, FL (April 2000)
120. US-Japan Joint Conference, "Hybrids 2000", Ithaca, NY (May 2000)
121. Argonne National Lab, Argonne, IL (June 2000)
122. WPAFB, Wright-Patterson, OH (July 2000)
123. Gordon Conference on Polymer Physics, New London, CT (July 2000)
124. 2<sup>nd</sup> International Conference on Ceramics, Boulder, CO (July 2000)
125. Department of Chemistry, University of Crete, Greece (October 2000)
126. SES 2000, Columbia, SC (October 2000)
127. Nanocomposites 2000 Conference, Brussels, Belgium (November 2000)
128. Institute of Electronic Structure & Lasers, Heraklion, Greece (November 2000)
129. Department of Chemistry, University of Athens, Greece (December 2000)
130. MRS Fall Meeting, Boston, MA (December 2000)

#### *Invited Seminars to Industry*

91. Dexter Electronics, Olean, NY (January 2000)

- 92. BP Amoco, Alpharetta, GA (February 2000)
- 93. Goodyear Co. Akron, OH (March 2000)
- 94. Cabot, Boyertown, PA (March 2000)
- 95. Nanocor, Arlington Heights, IL (March 2000)
- 96. Union Carbide, NJ (June 2000)
- 97. Southern Clay Products (July 2000)
- 98. Goodyear Co., Akron, OH (July 2000)
- 99. Goodyear Co., Akron, OH (December 2000)

#### **New Discoveries**

None

#### **Honors/Awards**

*1999 PEL Associates Award in Applied Polymer Chemistry*

Editorial Board, *Macromolecules*

Editorial Board, *Chemistry of Materials*

# Effect of Layer Charge on the Intercalation of Poly(ethylene oxide) in Layered Silicates: Implications on Nanocomposite Polymer Electrolytes

Juraj Bujdák,<sup>†</sup> Emily Hackett, and Emmanuel P. Giannelis\*

Department of Material Science and Engineering, Cornell University, Ithaca, New York 14853

Received October 22, 1999. Revised Manuscript Received May 19, 2000

The effect of layer charge on the intercalation of poly(ethylene oxide) (PEO) was investigated using a series of reduced-charge montmorillonites and smectites with varying layer charge. The amount of intercalated polymer initially increases with layer charge but then decreases. In contrast, the amount of water present continuously increases. This water is mostly coordinated with the gallery cations. When PEO is intercalated, it replaces water molecules filling the space between the hydrated exchangeable cations. Molecular simulations confirm the experiments and show that the polymer oxygen atoms do not directly associate with the exchangeable cations, which are mostly coordinated to water molecules and surface oxygen atoms.

## Introduction

Improvements in rechargeable, high-energy density batteries are key to the development of products ranging from zero-emission vehicles to portable electronics. A key unsolved problem is the design and implementation of lightweight, chemically stable, and environmentally benign electrolyte/electrode combinations. Of particular interest are Li salts dissolved in flexible polymers such as poly(ethylene oxide) (PEO). A serious drawback in these systems is the precipitous decrease in conductivity at temperatures below the melting temperature, which is typically above room temperature. One of the most promising ways to improve the electrochemical performance of polymer electrolytes is to form composite electrolytes by adding inorganic fillers.

Polymer nanocomposites represent a radical alternative to conventional composite electrolytes. Previously we reported a nanocomposite polymer electrolyte based on intercalated PEO in a layered silicate with room-temperature conductivity several orders of magnitude higher than that of LiBF<sub>4</sub>/PEO.<sup>1</sup> Polymer intercalation disrupts the normal, three-dimensional structure of the polymer chains and offers the means to suppress polymer crystallization. Furthermore, since the counteranions are the massive silicate layers, single-ion conduction is anticipated.

Intercalation of PEO in layered hosts, particularly in layered silicates, has been studied extensively.<sup>1–16</sup>

Proposed arrangements for the intercalated chains up to this point have been based mostly on X-ray diffraction studies and generally assume a highly ordered polymer arrangement within the host gallery.

One proposed structure for the intercalated PEO is a helix. In this model, the cations are located in the center of the helix and are coordinated to the oxygen atoms of the PEO similarly to crown ethers. This arrangement was favored on the basis of infrared and nuclear magnetic resonance measurements. However, recent NMR work does not support the crown-ether-like association between the cations and the PEO oxygen atoms.<sup>2</sup> Furthermore, a helical structure would not allow full interaction of PEO chains with the silicate surface.

A second suggestion is that the PEO chains are organized in two extended, all-trans layers parallel to the silicate surface. Again the cations are assumed to be drawn to the center of the host gallery and coordinated by PEO oxygen atoms. This highly ordered structure is improbable on the basis of energetic considerations. Additionally, the structure would be perturbed by the presence of the exchangeable cations, which are heterogeneously distributed according to the layer charge distribution. This perturbation is much

\* To whom correspondence should be addressed.

<sup>†</sup> Permanent address: Institute of Inorganic Chemistry, Slovak Academy of Sciences, SK-84236 Bratislava, Slovakia.

(1) Vaia, R. A.; Vasudevan, S.; Krawiec, W.; Scanlon, L. G.; Giannelis, E. P. *Adv. Mater.* **1995**, *7*, 154.

(2) Wong, S.; Vaia, R. A.; Giannelis, E. P.; Zax, D. B. *Solid State Ionics* **1996**, *86*, 547.

(3) Ruiz-Hitzky, E.; Aranda, P. *Adv. Mater.* **1990**, *2*, 545.

(4) Aranda, P.; Galvan, J. C.; Casal, B.; Ruiz-Hitzky, E. *Electrochim. Acta* **1992**, *37*, 1573.

(5) Aranda, P.; Ruiz-Hitzky, E. *Chem. Mater.* **1992**, *4*, 1395.

(6) Wu, J.; Lerner, M. M. *Chem. Mater.* **1993**, *5*, 835.

(7) Perfitt, R. L.; Greenland, D. J. *Clay Miner.* **1970**, *8*, 305.

(8) Krishnamoorti, R.; Vaia, R. A.; Giannelis, E. P. *Chem. Mater.* **1996**, *8*, 1728.

(9) Janex, M. L.; Audebert, R.; Champlain, V.; Counord, J. L. *Colloid Polym. Sci.* **1997**, *275*, 352.

(10) Van de Ven, T. G. M.; Alince, B. J. *Colloid Interface Sci.* **1996**, *181*, 73.

(11) Montarges, E.; Michot, L. J.; Lhote, F.; Fabien, T.; Villieras, F. *Clays Clay Miner.* **1995**, *43*, 417.

(12) Perfitt, R. L.; Greenland, D. J. *Clay Miner.* **1970**, *8*, 317.

(13) Vaia, R. A.; Sauer, B. B.; Tse, O. K.; Giannelis, E. P. *J. Polym. Sci. Polym. Phys.* **1997**, *35*, 59.

(14) Billingham, J.; Breen, C.; Yarwood, J. *Vib. Spectrosc.* **1997**, *14*, 19.

(15) Liu, Y. J.; Schindler, J. L.; DeGroot, D. C.; Kannewurf, C. R.; Hirpo, W.; Kanatzidis, M. G. *Chem. Mater.* **1996**, *8*, 525.

(16) Vaia, R. A.; Teukolsky, R. K.; Giannelis, E. P. *Chem. Mater.* **1994**, *6*, 1017. Vaia, R. A.; Jandt, K. D.; Kramer, E. J.; Giannelis, E. P. *Macromolecules* **1995**, *28*, 8080.



**Table 1. Cation Exchange Capacities of Reduced-Charge Montmorillonites**

sample	CEC (mmol/g)	(% of CEC <sub>M01</sub> )	sample	CEC (mmol/g)	(% of CEC <sub>M01</sub> )
Mo1	1.07	100	Mo5	0.71	66
Mo2	0.98	92	Mo6	0.52	49
Mo3	0.96	89	Mo7	0.24	22
Mo4	0.88	82	Mo8	0.11	10

greater when the hydration shell of the cations is taken into account. Fully replacing the water molecules in the coordination environment of the cations with less polar PEO oxygen atoms does not seem likely. PEO cannot play the role of a bridge in the electrostatic interaction between the cations and basal oxygen atoms of silicate, as water molecule dipoles may do.

In contrast to these proposals, some earlier reports have suggested that the gallery ions do not associate directly with PEO oxygen atoms and that their interaction with the polymer is mediated via the water molecules of their original hydration shells.<sup>7</sup> The above suggestions also do not take into account the heterogeneous nature of layered silicates such as layer charge density and ion location. These features give rise to hydrophobic and hydrophilic zones on the silicate surface. Thus, water and polymer molecules will absorb in these regions with varying affinity, producing a more disordered polymer structure than has been suggested so far.

In this paper we address the issues of cation coordination and silicate surface structure. We explore the effect of layer charge on PEO intercalation in layered silicates using a series of reduced charge montmorillonites and smectites. Additionally we focus on structure and interactions among the cation, the polymer, and the host surface and how these interactions affect the coordination shells of the cations.

### Experimental Section

Synthetic Li-fluorohectorite (FH) (Corning Inc.) was used as received. Saponite (SapCa-1, Clay Mineral Society, Source Clays) was purified by sedimentation. Na-saponite was prepared by reaction with excess NaCl solution.

High-charge montmorillonite SAz-1, middle-charge montmorillonites HD and JP, and low-charge montmorillonite M40A (Wyoming), nontronite SWa-1, and iron-rich beidellite ST, were obtained from the collection of the Institute of Inorganic Chemistry, Slovak Academy of Sciences (Bratislava, Slovakia). More information about the purification and properties of these samples has been published elsewhere.<sup>17,18</sup>

The reduced-charge montmorillonites (RCMs) were prepared as described previously.<sup>19</sup> Briefly montmorillonite (Jelšovský Potok, Slovakia) was first purified by sedimentation. The obtained dispersion of particles <2  $\mu$ m was repeatedly saturated with a lithium chloride solution, washed several times to remove excess salt, and dried before being heated to 100–200 °C. Through this heat treatment the Li cations are driven inside the silicate framework and become immobile and nonexchangeable. As a result a series of montmorillonites with reduced charge and well-controlled cation exchange capacity (CEC) but similar particle size can be produced. Table 1 lists the different RCMs prepared in this manner and their nominal charge.

Nanocomposites were prepared by solution or melt intercalation. PEOs with molecular weights (MWs), 7500 (Polysciences Inc.) and 100 000 and 5 000 000 (Aldrich) were used. For melt intercalation a mixture of PEO and the silicate host was ground and mixed for 2 min. Equal weights of PEO and silicate were used, which enabled full polymer saturation of the host with some excess polymer. Pellets were pressed using a hydraulic press at 450 MPa for 20 s and subsequently heated to various temperatures for 15 h. Polymer intercalation was monitored using X-ray diffraction (XRD).

Solution intercalation was accomplished by slowly adding a 0.25% aqueous solution of PEO to 50 mL of a 0.1% suspension of the silicate in water to a final polymer/silicate weight ratio of 1:1. The resulting dispersions were allowed to age for 3 days with occasional shaking. Nanocomposite films were prepared by drying a small amount of the resulting suspension on a glass slide. The remaining dispersion was centrifuged, and the excess polymer was washed away by repeated dispersion in distilled water and centrifugation. Samples were washed 10 times to remove all nonadsorbed polymer and dried under vacuum at 50 °C for 2 days. The amount of irreversibly adsorbed polymer was determined by thermogravimetric analysis (TGA).

XRD patterns were collected on a Scintag Inc. diffractometer equipped with an intrinsic germanium detector using Cu K $\alpha$  radiation. TGA was carried out on a Perkin-Elmer thermogravimetric analyzer (TGA 7) in air. A heating rate of 5 °C/min was used.

Canonical ensemble (NVT) computer simulations were performed using Cerius<sup>2</sup> software. The *d* spacing and polymer loading were input from XRD and TGA experiments, respectively. The simulation box parallel to the silicate layer measured 4.224 nm  $\times$  3.656 nm with periodic boundary conditions. Accurate force fields were adopted from literature studies of silicate hydration<sup>20,21</sup> and PEO/LiI mixtures.<sup>22,23</sup> These force fields have been carefully fit together to model this new system. Details of the simulation are given elsewhere.<sup>32</sup>

The amount of adsorbed water was determined by Monte Carlo simulations at 300 K. In these simulations a water vapor pressure of 100 kPa (1 atm) was imposed, and water was adsorbed through Grand Canonical Monte Carlo (GCMC) insertion, deletion, translation, and rotation trials. After water adsorption the system was equilibrated using molecular dynamic (MD) simulations. The water molecules were subsequently deleted and readsorbed through a second GCMC run to ensure thermodynamic equilibrium.

Water coordination to Li<sup>+</sup> was studied by considering the mass distribution plot of the entire GCMC simulation to

(17) Janek, M.; Komadel, P.; Lagaly, G. *Clay Miner.* **1997**, *32*, 623.  
 (18) Bujdák, J.; Janek, M.; Madejová, J.; Komadel, P. *J. Chem. Soc., Faraday Trans.* **1998**, *94*, 3487.  
 (19) Bujdák, J.; Komadel, P. *J. Phys. Chem. B* **1997**, *101*, 9065.

(20) Chan, Y. K. A Study of the Swelling of Sodium Montmorillonite by Molecular Simulations. Masters Thesis, Cornell University, Ithaca, NY, 1998.

(21) Chang, F. C.; Skipper, N. T.; Sposito, G. *Langmuir* **1997**, *13*, 2074.

(22) Smith, G. D.; Jaffe, R. L.; Yoon, D. Y. *J. Chem. Phys.* **1993**, *97*, 12752.

(23) Müller-Plathe, F. *Acta Polym.* **1994**, *45*, 259.

(24) Sposito, G.; Prost, R. *Chem. Rev.* **1982**, *82*, 553.

(25) Bujdák, J.; Petrovičová, I.; Slosiariková, H. *Geol. Carpathica, Ser. Clays* **1992**, *43*, 109. Komadel, P.; Bujdák, J.; Madejová, J.; Šucha, V.; Elsass, F. *Clay Miner.* **1996**, *31*, 333. Calvet, R.; Prost, R. *Clays Clay Miner.* **1971**, *19*, 175.

(26) Brindley, G. W.; Ertem, G. *Clays Clay Miner.* **1971**, *19*, 399. Ertem, G. *Clays Clay Miner.* **1972**, *20*, 199.

(27) Smith, K. L.; Van Cleve, R. *Ind. Eng. Chem.* **1958**, *50*, 12.

(28) Madorsky, S. L.; Straus, S. J. *Polym. Sci.* **1959**, *36*, 183. Fares, M. M.; Hacıoglu, J.; Suzer, S. *Eur. Polym. J.* **1994**, *30*, 845. Mantzavinos, D.; Livingston, A. G.; Hellenbrand, R.; Metcalfe, I. S. *Chem. Eng. Sci.* **1996**, *51*, 4219.

(29) Sposito, G.; Prost, R. *Chem. Rev.* **1982**, *82*, 571. Chang, F. C.; Skipper, N. T.; Sposito, G. *Langmuir* **1997**, *13*, 2074. Prost, R.; Koutit, T.; Benchara, A.; Huard, E. *Clays Clay Miner.* **1998**, *46*, 117.

(30) Van Olphen, H. *An Introduction to Clay Colloid Chemistry*; John Wiley & Sons: New York, 1963. Newman, A. C. D. *Chemistry of Clays and Clay Minerals*; Longman Scientific & Technical: London, 1987.

(31) Doner, H. E.; Mortland, M. M. *Soil Sci. Soc. Am. Proc.* **1971**, *35*, 360.

(32) Hackett, E.; Manias, E.; Giannelis, E. P. *Chem. Mater.* **2000**, *8*, 2161.

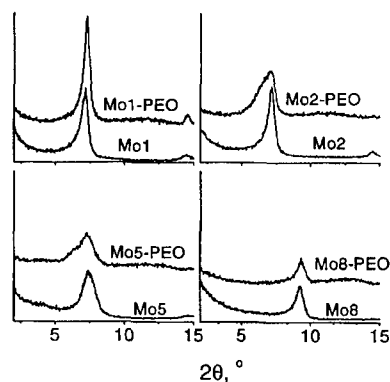


**Figure 1.** X-ray diffraction patterns of some reduced-charge montmorillonites and their unheated mixtures with poly(ethylene oxide) (MW 100 000).

ensure good statistics. The mass distribution was calculated in the projected plane parallel to the silicate walls. From this the number of Li ions coordinated to each water molecule was calculated.

### Results and Discussion

Figure 1 compares the XRD patterns of different RCMs and the corresponding PEO–RCM mixtures ( $MW_{\text{PEO}} = 100\,000$ ). The 001 basal reflection for the Mo1–Mo8 samples is in the range of 7–9°. The corresponding  $d_{001}$  value for the Mo1–Mo4 samples is about 1.2 nm.<sup>19</sup> Taking into account the montmorillonite layer thickness of 0.95 nm, the remaining corresponds to a monolayer of water molecules.<sup>24</sup> Further decrease of the layer charge (Mo5–Mo7) causes a nonswelling phase to appear. Mo8 contains only a nonswelling phase with a  $d$  spacing of 0.95 nm. In the others (Mo5–Mo7) a mixture of expandable and collapsed layers is present, evidenced by the broadening of the basal reflection. The number of collapsed layers in the mixed-layer structure (0.95/1.24 nm) increased gradually with decreasing charge (Mo5–Mo7).<sup>19,25</sup>

No apparent difference between the diffraction pattern of Mo1 and the PEO–Mo1 mixture was observed. On the other hand, a small change was observed for the mixtures containing the lower charge silicates (Mo2–Mo6). The reflections for these samples were broadened toward lower angles, i.e., higher interlayer distances. This change indicates partial but detectable intercalation of the polymer chains probably near the particle edges. Note the XRD patterns were obtained before any heating of the polymer/silicate mixtures. The collapsed layers, dominant in the structures of Mo7 and Mo8, remained unchanged in the presence of PEO. The same behavior was observed for the Mo7 and Mo8 samples under other intercalation conditions.

Heating at 60 °C (Figure 2a), which is still below the melting point of the bulk polymer ( $T_m = 66$  °C), led to polymer intercalation in Mo1–Mo6. As the layer charge of the RCMs decreased, the value of the basal spacing increased from 1.78 (Mo1) to 1.87 nm (Mo6), a small but reproducible difference. The  $d$  spacings correspond roughly to intercalation of two layers of PEO in the interlayer space. The small variations in the  $d$  spacing could be due to differences in the arrangement of the PEO chains. Alternatively a mixed-layer structure containing a polymer-intercalated phase and a phase

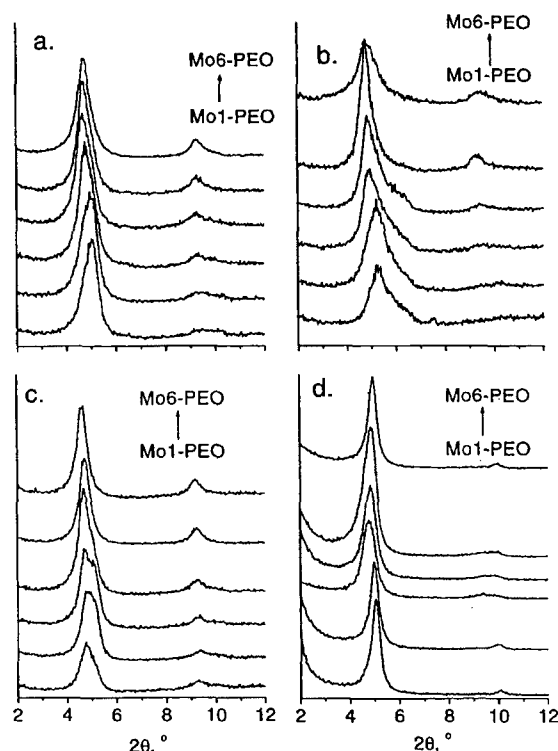


**Figure 2.** X-ray diffraction patterns of poly(ethylene oxide)-reduced-charge montmorillonite mixtures: (a) pellets with the polymer of MW 100 000, heated at 60 °C; (b) pellets with the polymer of MW 7500, at room temperature; (c) pellets with the polymer of MW 5 000 000, heated at 75 °C; (d) films with the polymer of MW 100 000, prepared from solution intercalation.

with lower spacing might be present. The presence of mixed-layer structure was supported by the absence of 002 reflections in Mo1 and Mo2 and only very-low-intensity peaks in the Mo3- and Mo4-containing samples. Further decrease in layer charge (Mo5, Mo6) results in a more uniform hybrid structure characterized by relatively intense and narrow diffraction peaks. The collapsed phase found in pure Mo5 and Mo6 was reexpanded partially in the presence of the polymer. The ability of many polar organic compounds (glycol, glycerol, ethanol, etc.) to expand a nominally nonswelling interlayer in water has been previously reported.<sup>26</sup>

Similar trends were observed in the intercalation of low MW PEO (7500) at room temperature (Figure 2b), and of very high MW PEO ( $5 \times 10^6$ ) at 75 °C (Figure 2c). Intercalation of low MW PEO takes place even at room temperature due to the higher mobility of relatively small PEO chains (Figure 2b). The broad band of the Mo6–PEO hybrid (Figure 2b) may indicate the presence of a collapsed phase, which is not fully re-opened by polymer intercalation at low temperatures. Finally the same dependence of the  $d$  spacing on layer charge was also observed in the samples prepared by solution intercalation (Figure 2d).

High molecular weight PEO (5 000 000) was not completely intercalated in some cases (Mo1–Mo4), even when heated for 15 h at 75 °C, which is above the melting point of this polymer (Figure 2c). PEO with very long chains forms high-viscosity melts even at temperatures much higher than its melting point.<sup>27</sup> Such a high viscosity could hinder the intercalation of the

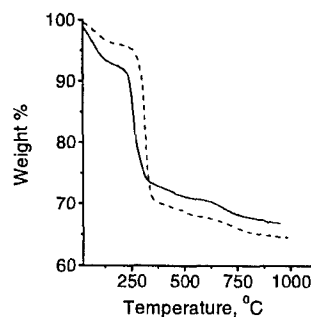


**Figure 3.** Thermogravimetric analysis of Mo1-PEO (solid line) and Mo5-PEO (dashed line).

polymer into the interlayer spaces of the inorganic host.

The trends observed above (Figure 2) could be summarized as follows. A mixed-layer structure containing a polymer intercalated phase corresponding to roughly two polymer layers and a phase with lower spacing (one layer of PEO chains and/or a nonintercalated phase) is formed in the high-charge silicates. A more uniform interlayer structure is present as the layer charge decreases. Additionally, the *d* spacing increases with decreasing layer charge.

TGA was used to quantify the amount of intercalated PEO and water present in the nanocomposites. Aranda and Ruiz-Hitzky<sup>4</sup> found very good agreement between the amounts of PEO adsorbed on layered silicates determined by TGA and organic content microanalysis. For these measurements samples prepared via solution intercalation were used.

PEO decomposes at temperatures above 300 °C, forming monomers, small oligomers, and other decomposition products.<sup>28</sup> Thermal decomposition of PEO nanocomposites proceeds as a multiple-step process: (1) weight loss due to the release of water (<225 °C); (2) decomposition of the polymer (225–400 °C); (3) dehydroxylation of montmorillonite at about 700 °C. Representative TGA traces of two nanocomposites, PEO-Mo1 (solid line) and PEO-Mo5 (dashed line), are shown in Figure 3. Both the release of water and the decomposition of the polymer shift to higher temperature for the Mo5-containing sample. Judging from the weight losses, the Mo5-PEO hybrid contains less water but more polymer compared to the corresponding Mo1 hybrid.

Figure 4 shows the amount of water and PEO as a function of the layer charge or CEC. The amount of PEO initially increases with CEC, but it reaches a maximum. On the other hand, the amount of adsorbed water continuously increases with CEC but does not exceed 10% of the total weight. Normally the amount of water in the silicate before polymer intercalation can be as high as 20%. This suggests that PEO, when adsorbed on the silicate surface, replaces water in agreement with previous observations.<sup>3,6,7,12</sup> Low contents of PEO and water in the Mo7 and Mo8 samples could be explained by the presence of collapsed interlayers, in which less surface area is accessible for intercalation.

The increase of the water content in PEO-RCMs with CEC indicates that water remaining after polymer intercalation is mainly associated with the exchangeable cations and is part of their hydration shells. Therefore,

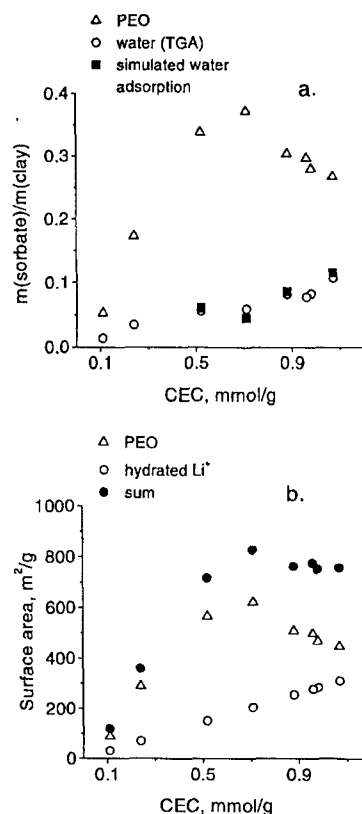


**Figure 4.** Relationships between the amounts of water and PEO adsorbed from water dispersions and the cation exchange capacity of montmorillonite: (a) weights of adsorbed PEO and water; (b) surface areas occupied by PEO and hydrated Li<sup>+</sup> cations.

PEO does not coordinate directly with the exchangeable cations. If complexation with the cations is necessary for PEO intercalation, then the decrease of the layer charge, or CEC, would lead to less intercalated polymer. The opposite was observed for fully expanded RCMs (Mo1–Mo5). Reducing the number of hydrated cations frees up more silicate surface, allowing more polymer to be intercalated. In contrast, in high CEC silicates, the amount of hydrated cations hinders polymer intercalation. Exchangeable cations are in fact the only strongly hydrophilic sites on the silicate surface,<sup>29</sup> and the water bound to these cations is released only at relatively high temperatures. On the other hand, basal Si–O groups in the spaces between hydrated cations in the interlayers are relatively hydrophobic. PEO is more hydrophobic than water and is preferentially adsorbed on these sites. It does not require replacement of the water from the hydration shell of the cations. The existence of two kinds of water and their different contents in RCMs are supported by differential thermogravimetry (DTG) (Figure 5). Water was released from the RCMs in two steps with increasing temperature as shown by two representative examples (Mo1, Mo5). The amount of relatively weakly bound water (released below 100 °C) was higher in Mo5 (about 16.5% compared to 12% in Mo1). In contrast Mo1 contained relatively more water coordinated to the cations than Mo5 (about 6% and 3%, respectively). This water was released at temperatures above 100 °C.

The CEC values and experimentally measured amounts of PEO were used to estimate the surface area

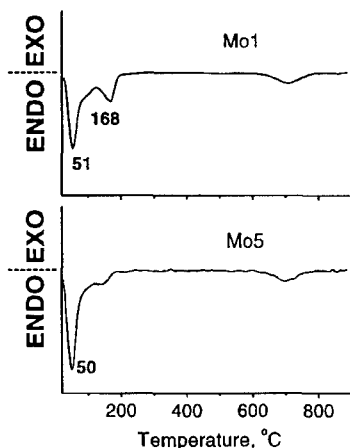


Figure 5. Differential thermogravimetry of Mo1 and Mo5 samples.

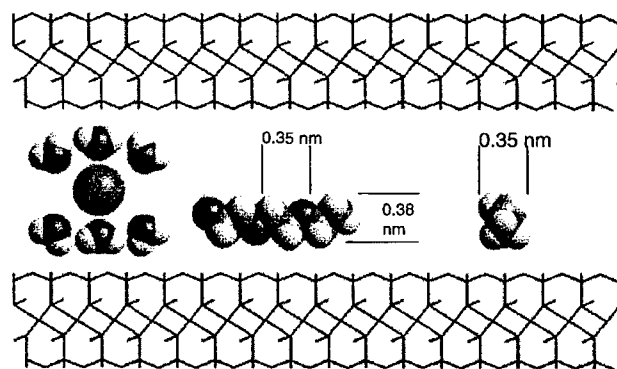


Figure 6. Schematic showing coordination of  $\text{Li}^+$  by water molecules (left), the length (0.35 nm) of an all-trans PEO monomer (center), and the width (0.38 nm) of an all-trans PEO chain (right).

occupied with hydrated  $\text{Li}^+$  cations and polymer chains, respectively. For each  $\text{Li}^+$  cation, an octahedral complex with the plane of three water molecules parallel to the silicate surface was considered (Figure 6). Such a complex would occupy  $0.48 \text{ nm}^2$  ( $0.24 \text{ nm}^2$  for each layer).<sup>29</sup>

The dimensions of zigzag chains of PEO containing only trans bonds are 0.38 and 0.35 nm, respectively, while the length of the monomeric unit  $-\text{C}_2\text{H}_4-\text{O}-$  is 0.35 nm (Figure 6). Also recall that the observed  $d$  spacing corresponds to two layers of polymer chains. Therefore, each monomeric unit of adsorbed PEO occupies only one of two layers, and the area is  $(0.35 \text{ nm})^2 = 0.12 \text{ nm}^2$ . The presence of gauche conformations would affect the value of the surface occupied by the polymer, but not significantly. Therefore, this arrangement was neglected. In the calculations we assumed that all the water molecules are associated with  $\text{Li}^+$  ions and that water molecules are not shared between  $\text{Li}^+$  ions. We also assumed that all the cations and the polymer reside in the galleries and not on particle edges. The calculated surface area occupied by hydrated  $\text{Li}^+$  cations and polymer chains, with respect to the CEC and the amount of adsorbed polymer, is presented in Figure 4b. The area occupied by hydrated  $\text{Li}^+$  ions increases with CEC and is about  $300 \text{ m}^2/\text{g}$  for the highest charge samples. On the other hand, the area covered by polymer chains is always higher than that

Table 2. Amounts of PEO and Water Adsorbed from Water Solution on Smectites, As Determined by Thermogravimetry

smectite	water amount (%)	PEO amount (%)	Smectite	water amount (%)	PEO amount (%)
FH	5.1	0.0	SWa-1	2.5	16.2
ST	8.8	11.4	JP	5.4	19.2
SAz-1	9.9	11.4	M40A	4.2	22.2
HD	7.3	13.3	saponite	4.2	22.1

covered by the cations and their hydration shells, and it goes through a maximum. While this difference is not as large in the case of PEO-Mo1, the area covered by the polymer increases (for fully expandable RCMs) and that of hydrated cations decreases with decreasing CEC. In the case of Mo5-Mo7 the surface covered with polymer is more than 3 times that occupied by hydrated cations. That this model provides a good estimate despite its simplicity is evidenced by the excellent agreement between the overall surface (near  $800 \text{ m}^2/\text{g}$ ) of the expandable RCMs (Mo1-Mo6) and that calculated from the unit-cell dimensions and determined by other methods.<sup>30</sup>

The trends observed in the RCMs were confirmed using Na-smectites of different composition and layer charge. The layer charge of these silicates, determined by the alkylammonium method, decreases in the order  $\text{ST} \approx \text{SAz-1} > \text{HD} > \text{SWa-1} > \text{JP} > \text{M40A}$ .<sup>17,18</sup> The amounts of PEO and water present (Table 2) were compared together with those of two reference samples, very-high-charge, synthetic fluorohectorite and low-charge trioctahedral smectite-saponite. No PEO was intercalated on FH, or if it was, it was subsequently washed away with water, suggesting a very weak adsorption. The amount of adsorbed water was also relatively low (5.1%). Due to the very high cation density on FH, hydrated exchangeable cations occupy the majority of the surface and, hence, hinder PEO intercalation. The small amount of water present could be due to lower expandability of this silicate, which is common for high-charge smectites<sup>31</sup> and/or the high cation density. The hydration shells of some neighboring cations may not be fully saturated and may share water molecules. High-charge SAz-1 and ST intercalated a relatively small amount of PEO (about 11.5%) and retained a high amount of water (10% and 8.9%, respectively). Lowest charge montmorillonite M40A and low-charge saponite contained the highest amount of PEO. However, the amount of water remaining on the clay surface depends not only on the layer charge of smectite and the number of exchangeable cations, but also on the layer charge location, controlling the expandability of the smectite.<sup>31</sup> Relatively lower water amounts were observed for the tetrahedrally charged silicates (ST vs SAz-1; SWa-1 vs JP).

The amount of water present on PEO-RCMs calculated by computer simulations agrees well with the experimental values and trends, confirming the accuracy of the force field (Figure 4). The simulations also show that the intercalated polymer chains form two discrete layers, but the polymer retains a disordered, liquidlike structure.<sup>32</sup> This layering of molecules in confinement has been observed previously both experimentally<sup>33</sup> and in computer simulations.<sup>34</sup>

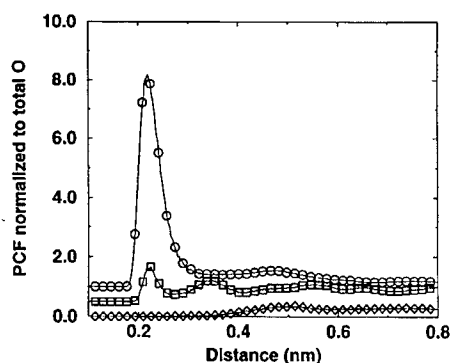


**Figure 7.** Radial pair correlation functions for oxygen atoms in the silicate/PEO nanocomposite (CEC = 1.05 mmol/g): (circles) water oxygen atoms, shifted up 1.0 for clarity, coordination number (CN) = 5.47; (squares) silicate surface oxygen atoms, shifted up 0.5 for clarity, CN = 1.10; (diamonds) PEO oxygen atoms, CN = 0.05. The overall CN (6.2) is equal to the sum of CNs of water, PEO, and silicate oxygen atoms.

More detailed information on the interactions of  $\text{Li}^+$  cations with oxygen atoms of PEO, water, or the silicate surface is obtained from the radial pair correlation functions (PCFs). The PCF records the average coordination environment of an atom. In the bulk the probability of finding an atom at an arbitrary point is proportional to the density of the medium. By extension, the probability that an atom will be found at distance  $r$  from a particular point is proportional to the density of the medium. The PCF of this arbitrary point, normalized to the bulk, would therefore be one for all distances  $r$ . If the point represented an atom of finite size, other atoms would be excluded from the space that it occupies. Consequently, the PCF or the probability of finding an atom at distance  $r$  from the test atom would be 0 for  $r$  less than the sum of the two radii. If other atoms coordinate to the central atom, then the local density in a spherical shell just beyond that atom would be greater than the average density of the medium. The PCF, normalized to the bulk density, at the corresponding  $r$  would have a peak with a value greater than 1. Steric ordering around the coordination shell may cause a second, weaker peak approximately one atomic diameter from the first. However, for large  $r$ , the effect of the central atom would no longer be felt and the PCF would approach a constant value of 1. In summary, a typical PCF has a value of 0 for  $r$  less than one atomic diameter, at least one peak due to coordination and local ordering around the central atom, and a value of 1 at longer distances, due to the normalization against bulk density.

The PCFs in Figure 7 illustrate the degree of association between the  $\text{Li}^+$  cations and oxygen atoms from water, PEO, and the silicate surface. The PCFs are normalized against the *total* oxygen atom density in the gallery (excluding the inner layers of the silicate crystal), so that the sum of all PCFs shown in Figure 7 approaches one at large distances, as described above. Since PCFs effectively measure the average local density, they can be integrated to yield the average number

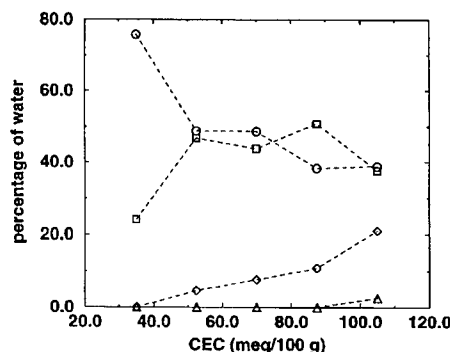


**Figure 8.** Percentage of absorbed water molecules calculated from computer simulations (accepted MC insertions) which do not coordinate  $\text{Li}^+$  ions (circles), or within a distance of 3.5 Å from one (squares), two (diamonds), or three (triangles)  $\text{Li}^+$  ions.

of atoms in a sphere around a central atom ( $\text{Li}^+$  ion in this case). From the PCFs it is clear that the cations are principally coordinated to water molecules and that the PEO is further away from the cations. In addition, the cations partially associate with the silicate surface while PEO resides outside the coordination shell of the cations. The second peak in the silicate surface oxygen PCF is due to the periodic crystal structure of the montmorillonite.

From the mass distribution of the GCMC simulations the coordination of the water molecules can be further analyzed (Figure 8). As the CEC increases the amount of water which does not coordinate any  $\text{Li}^+$  decreases. The amount, which coordinates a single  $\text{Li}^+$  ion, increases at first, leveling out or even falling slightly when it reaches about 50%. At the same time, the amount of water coordinated to two  $\text{Li}^+$  ions increases steadily. Only at the highest CEC does any water molecule coordinate with more than two  $\text{Li}^+$  ions at the same time. These trends reflect the increased concentration of the  $\text{Li}^+$  ions and the need for the water to coordinate to the ions within the constraints of the confined, polymer-filled space.

The computer simulations fully support the model suggested above on the basis of the experimental data. PEO intercalates by replacing predominantly free water molecules in the gallery rather than directly coordinating to the cations, which seem to maintain their hydration shell intact.

## Conclusions

Melt or solution intercalation of PEO into layered silicates leads to essentially identical structure in the nanocomposite. Experimental measurements coupled with computer simulations show that polymer chains replace weakly adsorbed water filling the space between hydrated exchangeable cations. No direct association between exchangeable cations and PEO oxygen atoms takes place. The amount of polymer adsorbed is controlled by the layer charge density, i.e., the surface area covered by the hydrated cations vs the surface area covered by weakly adsorbed water. The trends observed in this study may be applied to the intercalation/adsorption of layered silicates with other polymers<sup>35</sup> or organic compounds. For example, the lower expandabil-

(33) Christenson, H. K.; Gruen, D. W. R.; Horn, R. G.; Israelachvili, J. N. *J. Chem Phys.* **1987**, *87*, 1834.

(34) Hackett, E.; Manias, E.; Giannelis, E. P. *J. Chem Phys.* **1998**, *108*, 7410.

(35) Hetzel, F.; Doner, H. E. *Clays Clay Miner.* **1993**, *41*, 453.

ity of high-charge smectites and vermiculites in organic solvents such as ethylene glycol and glycerol<sup>36</sup> is probably due not only to higher attractive electrostatic forces but also to the high density of hydrated exchangeable cations and the lack of accessible surfaces for adsorption.

---

(36) Theng, B. K. G. *The Chemistry of Clay-Organic Reactions*; Halsted Press: New York, 1974.

**Acknowledgment.** This work was supported by AFOSR. E.H. acknowledges an NSF Graduate Research Fellowship. We thank E. Manias for helpful discussions. Partial support by the Slovak Grant Agency VEGA (Grant No. 2/4042/99) is also acknowledged.

CM990677P

# Computer Simulation Studies of PEO/Layer Silicate Nanocomposites

E. Hackett, E. Manias,\* and E. P. Giannelis†

Department of Materials Science and Engineering, Cornell University, Ithaca, New York 14853

Received October 22, 1999. Revised Manuscript Received April 4, 2000

Monte Carlo and molecular dynamics computer simulations are used to explore the atomic scale structure and dynamics of intercalated PEO/montmorillonite nanocomposites. Particular attention is paid to the configuration of the polymer within these confined spaces. A layered, but disordered and liquid-like, structure is observed, in contrast to the all-trans or helical extended interlayer structures traditionally suggested. The cations primarily reside near the silicate surface. Molecular dynamics simulations also provide information on the interlayer mobility of  $\text{Li}^+$  ions, which is related to the ionic conductivity in polymer electrolyte nanocomposites.

## I. Introduction

Nanocomposites composed of poly(ethylene oxide) (PEO) intercalated between the layers of mica-type silicates represent a new class of polymer composite electrolytes.<sup>1–9</sup> They possess novel mechanical and electrical properties that render them very promising materials for applications such as solid-state lithium batteries. A better understanding of the structure and dynamics of the intercalated polymers in these nanocomposites can provide molecular insight and lead to the design of materials with improved properties.

Mica-type layer silicates share the same structural characteristics as the better known talc and mica. Their crystal lattice consists of negatively charged aluminosilicate layers. These layers are negatively charged, and in their pristine form this charge is balanced by hydrated cations ( $\text{Li}^+$ ,  $\text{Na}^+$ , or  $\text{Ca}^{2+}$ ) that occupy the spaces between the layers (galleries). PEO can be intercalated, or inserted, between these layers by replacing, partly or completely, the water molecules occupying the interlayer. This can be accomplished by melt intercalation, in which a dry PEO/silicate mixture is heated above the melting temperature ( $T_m$ ) of the PEO, at which point it spontaneously intercalates as observed by X-ray diffraction.<sup>5</sup> Alternatively, the nano-

composite can also be prepared from an aqueous solution,<sup>4,6</sup> resulting in nanocomposite structures similar to those prepared by the melt intercalation method. In the nanocomposites, PEO forms the matrix for a solid state electrolyte whose conductivity is primarily cationic because the anions are the large silicate layers. Furthermore, the intercalated polymers of the nanocomposite do not exhibit any marked melting transition near the bulk  $T_m$  of PEO, and at temperatures below  $T_m$ , they promote much higher cationic conductivities than the respective bulk PEO/alkali systems. In addition, the polymer chains in the nanocomposite show significant mobility, even at temperatures well below the bulk  $T_m$ .<sup>5</sup>

The polymer chains and silicate layers self-assemble in an alternating fashion with a periodic  $d$  spacing of  $18 \pm 1$  Å, of which 9.7 Å corresponds to the silicate layer.<sup>4,6</sup> The polymer chains are confined within  $8 \pm 1$  Å, only a few atomic diameters wide. This extreme confinement has a profound effect on the structure of the intercalated polymer. Additionally, the interactions between the alkali cations, the negatively charged silicate layers, and the polymer are important in understanding the structure of the nanocomposite as well as its conductivity. In addition, recent work<sup>6</sup> has shown that a small amount of water is present in the nanocomposite galleries when PEO is intercalated from solution. The computer simulations presented here study first the structure at the atomic level of intercalated PEO nanocomposites. Molecular dynamics simulations provide insight into the mobility of  $\text{Li}^+$  ions and the role that the cations' hydration shells plays in the cation conductivity. Dry and hydrated nanocomposites were studied and the effects of hydration on the structure and cation mobility are discussed.

## II. Model

All simulations were performed using Cerius<sup>2</sup> software, although most of the data analysis utilized programs developed especially for this nanocomposite system. The force fields used in this simulation study are based on a geometrically fitted and optimized

\* Current address: Department of Materials Science and Engineering, The Pennsylvania State University, 310 Steidle Bldg., University Park, PA 16802. E-mails: eh42@msc.cornell.edu; manias@psu.edu; epg2@cornell.edu.

(1) Aranda, P.; Ruiz-Hitzky, E. *Chem. Mater.* **1992**, *4*, 1395–1403.  
(2) Ruiz-Hitzky, E.; Aranda, P. *Adv. Mater.* **1990**, *2*, 545.  
(3) Aranda, P.; Galvan, J. C.; Casal, B.; Ruiz-Hitzky, E. *Electrochim. Acta* **1992**, *37*, 1573.

(4) Wu, J.; Lerner, M. M. *Chem. Mater.* **1993**, *5*, 835–838.  
(5) Wong, S.; Vaia, R. A.; Giannelis, E. P.; Zax, D. B. *Solid State Ionics* **1996**, *86*, 547–57.

(6) Bujdak, J.; Hackett, E.; Giannelis, E. P. *Chem. Mater.* **2000**, *8*, 2168.

(7) Vaia, R. A.; Vasudevan, S.; Krawiec, W.; Scanlon, L. G.; Giannelis, E. P. *Adv. Mater.* **1995**, *7*, 154.

(8) Vaia, R. A.; Sauer, B. B.; Tse, O. K.; Giannelis, E. P. *J. Polym. Sci. Polym. Phys.* **1997**, *35*, 59.

(9) Hutchison, J. C.; Bissessier, R.; Shriver, D. F. *Chem. Mater.* **1996**, *8*, 1597–1599.

combination of force fields used in previous studies of hydrated montmorillonite<sup>10–12</sup> and PEO–salt systems.<sup>13,14</sup> Silicate atoms have been completely constrained in all cases. Monte Carlo absorption simulations were carried out using an MCY water model with an offset oxygen charge, while for molecular dynamics (MD) simulations a modified MCY model in which the charge was centered at the atom centers produced adequate results.

The cation exchange capacity (CEC), which is a characteristic of the silicate and provides the charge on the silicate layers, determines the number of compensating cations in the gallery. The CEC of the silicates studied here is set to  $\approx 105$  mequiv/100 g. This is a common CEC for montmorillonite,<sup>31</sup> and corresponds to the silicate studied in the experimental counterpart to this work.<sup>6</sup> The simulation box uses periodic boundary conditions and is  $42.24 \times 36.56$  Å in the direction parallel to the silicate, while the third dimension is determined by the periodic repeat distance, or  $d$  spacing, which is measured by X-ray diffraction.

A  $d$  spacing of 18 Å was used for the  $\text{Li}^+$ –montmorillonite/PEO nanocomposite. After MD simulations of up to 50 000 time steps (0.1 ns) of the dry  $\text{Li}^+$ –montmorillonite/PEO system, which served to equilibrate the polymer configuration and provide structural information for the dry system, water was adsorbed through a grand canonical Monte Carlo (GCMC) simulation in which chemical equilibrium was established by imposing a water vapor pressure of 100 kPa (1 atm). The hydrated system was equilibrated with further MD simulation in an NVT ensemble. The water molecules were subsequently deleted and readsorbed through a second GCMC run that ensured an accurate amount of adsorbed water. The amount of water from these simulations is in very good agreement with the amount of water measured experimentally,<sup>6</sup> providing a useful check on the validity of the force field used here. After the water was adsorbed, several NVT MD simulations of up to 500 000 time steps (1 ns), at a temperature of 300 K, were carried out from various initial system configurations. Configurations were saved every 500 steps, and the stored trajectories were used to calculate the equilibrium structure and dynamic information presented here.

In the case of  $\text{Na}^+$ –montmorillonite, a  $d$  spacing of 17.6 Å was used. Several productive simulation runs, typically of 50 000 time steps (0.1 ns), were carried out from various initial configurations.

### III. Results and Discussion

A snapshot of the hydrated  $\text{Li}$ –montmorillonite system is shown in Figure 1. Although this is a snapshot of a particular water-containing system, it illustrates many of the features, discussed in detail below, that are

apparent in both dry and hydrated systems. These features include the preferred locations of ions and the disordered bilayer structure of the polymer.

Number density profiles showing the arrangement of  $\text{Li}^+$  or  $\text{Na}^+$  and polymer in the silicate gallery of the dry systems through a plane normal to the silicate surfaces are shown in Figure 2. Both the oxygen and carbon density profiles as well as the profiles of the polymer as a whole indicate a bilayer structure, with the thickness of each layer approximately equal to a PEO chain width as calculated from the known molecular structure. Such layer structures originate from the oscillating solvation forces near a surface. Their existence is suggested by several experimental and computer studies of nanoscopically confined fluids and polymers<sup>15–23</sup> including previous experimental observations of PEO intercalated in layer silicates that imply the existence of one or two intercalated layers.<sup>1–9</sup> In this layer structure confined chain molecules tend to align themselves parallel to the wall so that large segments of a chain will lie within a single layer, which is seen as a peak in the density profile (Figure 2). At the same time, the polymer chains are relatively disordered in the plane parallel to the silicate surface. Chains may twist around each other or span across the polymer layers within the gallery. Despite the layered ordering normal to the surfaces, the polymer configurations exhibit a disordered, almost liquid-like, structure. These findings contrast previous suggestions in which an all-trans extended bilayer or a helical structure for the polymer was proposed.<sup>1</sup>

The cations for both dry systems are bound to the wall (Figure 2), about 1.5 Å from the center of the surface oxygen atoms, or about 4.8 Å from the central plane of metal atoms, in very good agreement with NMR data.<sup>29</sup> Surface lattice cavities are characteristic of the oxygen network in all 2:1 layer silicates, and the cations primarily reside partially inserted within these cavities. Although the  $\text{Li}^+$  ions are smaller than the  $\text{Na}^+$  ions and their density profiles extend into the surface cavities, the  $\text{Li}^+$  density profiles have their largest peaks slightly outside these cavities (Figure 2). The cations' locations, as revealed by the simulations, contrast with the assumption that the cations are located in the middle of the gallery.<sup>1</sup> In addition, this agrees with the location of cations as shown in NMR data.<sup>29</sup> The location

(10) Chang, F. C.; Skipper, N. T.; Sposito, G. *Langmuir* **1997**, *13*, 2074–2082.

(11) Skipper, N. T.; Chang, F. C.; Sposito, G. *Clays Clay Miner.* **1995**, *43*, 285–293.

(12) Manias, E.; Chan, Y. K.; Giannelis, E. P.; Panagiotopoulos, A. Z.; Zax, D. B. CMS Workshop Lectures, The Clay Minerals Society, in press.

(13) Muller-Plathe, F. *Acta Polym.* **1994**, *45*, 259–293.

(14) Smith, G. D.; Jaffe, R. L.; Yoon, D. Y. *J. Phys. Chem.* **1993**, *97*, 12752–12759.

(15) Horn, R. G.; Israelachvili, J. N. *J. Chem. Phys.* **1981**, *75*, 1400.

(16) Christenson, H. K. *J. Chem. Phys.* **1983**, *78*, 6906.

(17) Chan, D. Y. C.; Horn, R. G. *J. Chem. Phys.* **1985**, *83*, 5311.

(18) Israelachvili, J. N.; Kott, S. J. *J. Chem. Phys.* **1988**, *88*, 7162.

(19) Montfort, J. P.; Hadzioannou, G. *J. Chem. Phys.* **1988**, *88*, 7187–96.

(20) Gee, M. L.; McGuigan, P. M.; Israelachvili, J. N.; Homola, A. M. *J. Chem. Phys.* **1990**, *93*, 1895–906.

(21) Israelachvili, J. *Intermolecular and Surface Forces*, 2nd ed.; Harcourt, Brace, Jovanovich: New York, 1992.

(22) Ribarsky, M. W.; Landman, U. *J. Chem. Phys.* **1992**, *97*, 1937.

(23) Xia, T. K.; Ouyang, J.; Ribarsky, M. W.; Landman, U. *Phys. Rev. Lett.* **1992**, *69*, 1967.

(24) Bitsanis, I. A.; Pan, C. J. *J. Chem. Phys.* **1993**, *99*, 5520.

(25) Gupta, S.; Koopman, D. C.; Westermann-Clark, G. B.; Bitsanis, I. A. *J. Chem. Phys.* **1994**, *100*, 8444.

(26) Padilla, P.; Toxvaerd, S. *J. Chem. Phys.* **1994**, *101*, 1490.

(27) Manias, E.; Hadzioannou, G.; ten Brinke, G. *Langmuir* **1996**, *12*, 4587.

(28) Hackett, E.; Manias, E.; Giannelis, E. P. *J. Chem. Phys.* **1998**, *108*, 7410.

(29) Yang, D.-K.; Zax, D. B. *J. Chem. Phys.* **1999**, *110*, 5325.



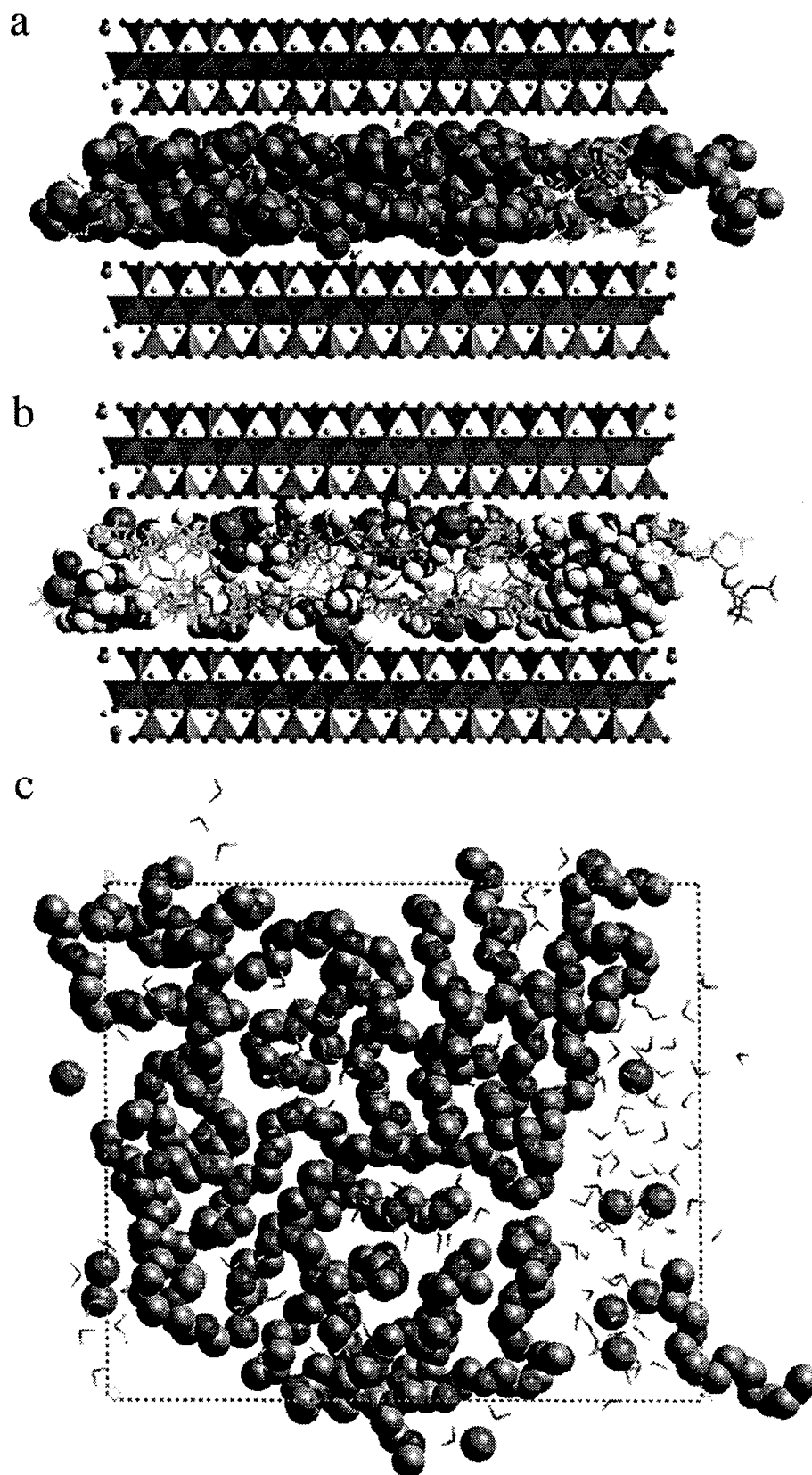


**Figure 1.** Snapshot of PEO-silicate nanocomposite: (a) showing the silicate crystal as polyhedra,  $\text{Li}^+$  as spheres, and highlighting PEO as spheres; (b) showing the silicate crystal as polyhedra,  $\text{Li}^+$  as spheres, and highlighting water as spheres; (c) top view with silicate removed, showing PEO and  $\text{Li}^+$  as spheres and water as sticks.

of the cations in the interlayer gallery becomes very important for these materials because, as will be discussed below, it affects the cationic mobility.

Density profiles for the hydrated PEO/ $\text{Li}^+$ -montmorillonite system are shown in Figure 3, corresponding to the snapshot of the system shown in Figure 1. The

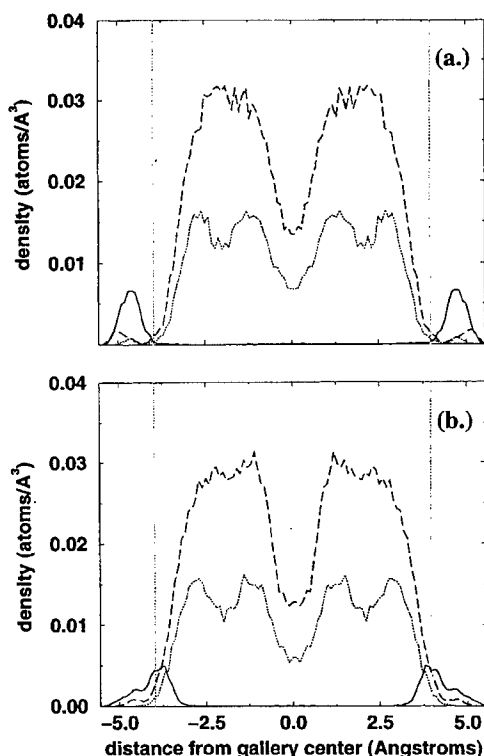


**Figure 2.** Density profiles normal to the silicate layers for (a) Na<sup>+</sup>-montmorillonite and (b) Li<sup>+</sup>-montmorillonite PEO nanocomposites. Solid line, cation (Na<sup>+</sup> or Li<sup>+</sup>); dotted line, PEO oxygen; dashed line, PEO carbon. Left and right graph boundaries correspond to the plane containing the centers of the surface oxygen atoms; pale gray vertical lines represent the outer edge of the surface oxygen layer. The pale gray dotted horizontal line represents the average atomic carbon density of bulk PEO as calculated from a handbook density for the bulk polymer (1.1 g/cm<sup>3</sup>).

bilayer structure of the polymer in this system is even more pronounced, and the disordered nature of the chain configurations can be seen clearly from the snapshot (Figure 1). Again, the liquid-like structure contrasts with previous suggestions of helical or all-trans extended polymer structures within the gallery.<sup>1</sup>

The observed configurations are also in very good agreement with small-angle neutron scattering (SANS) experiments. SANS profiles from 15 K to room temperature can only be simulated by assuming a disordered polymer configuration.<sup>30</sup> Integration of the density profiles (Figure 3) shows that slightly more than half of the ions reside in layers very near the silicate surface (<2.5 Å from the surfaces).

The density profile of Li inside the interlayer gallery of the hydrated system is quite different than that of the dry Na or Li systems. As before, some Li ions are located <2 Å from the surface, partially inserted within the surface lattice cavities, but now there also exists a large number of Li ions inside the galleries. They form two diffuse layers as the density profiles show (Figure 3).

In the long simulation of the hydrated system, few atoms were exchanged between the surface layers and gallery center over the time scale of this simulation (1

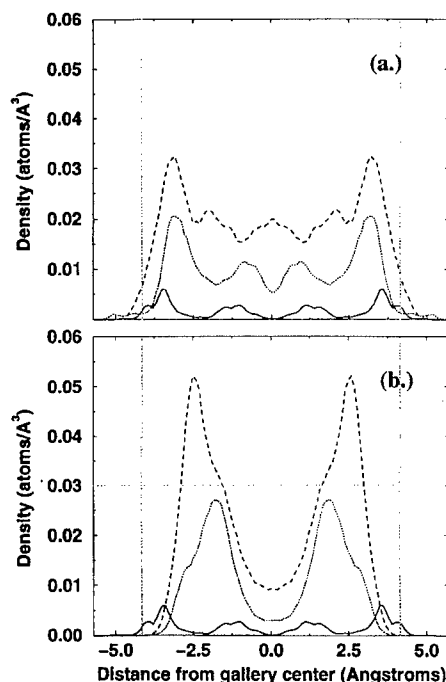


**Figure 3.** Density profiles within the silicate gallery for the hydrated Li<sup>+</sup>-montmorillonite/PEO nanocomposite: (a) Solid line, Li<sup>+</sup>; dotted line, water oxygen; dashed line, water hydrogen. (b) For the same systems as those in (a): solid line, Li<sup>+</sup>; dotted line, PEO oxygen; dashed line, PEO carbon. Left and right graph boundaries correspond to the plane containing the centers of the surface oxygen atoms; pale gray lines represent the outer edge of the surface oxygen layer.

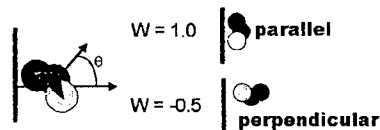


**Figure 4.** Schematic diagram of an idealized C-C-O bond and the silicate surface illustrating the definition of  $\theta$  used in the calculation of the order parameter and the bond configurations corresponding to the upper and lower limits of possible values for the order parameter.

ns). The small, outer shoulder of this first density peak is due to ions that have dropped into the crystalline cavities of the silicate surface. The water density profiles have a similar shape to the Li<sup>+</sup> density profiles, with the exception of this outer shoulder, suggesting that the water predominantly exists in hydration shells around the Li<sup>+</sup> ions, as can be directly observed from the system configurations through radial pair correlation functions (PCF), which are discussed below. In contrast, PEO density maxima occur between the minima where the Li<sup>+</sup> and water densities are relatively low, almost in the same positions as those in the dry systems but characterized here by narrower layer widths.

An order parameter can be defined that describes the orientation of the PEO bond angles.<sup>22-27</sup> If  $\theta$  is the angle between the normal to the plane formed by a C-C-O bond and a normal to the silicate surface, as illustrated schematically in Figure 4, an order parameter,  $W$ , can be defined as

$$W = \frac{1}{2} \langle 3 \cos^2 \theta - 1 \rangle \quad (1)$$

(30) Krishnamoorti, R. K.; Giannelis, E. P. unpublished data.

(31) Solomon, D. H.; Hawthorne, D. G. *Chemistry of Pigments and Fillers*; Kreiger Publishing Co.:Malabar, FL, 1991.

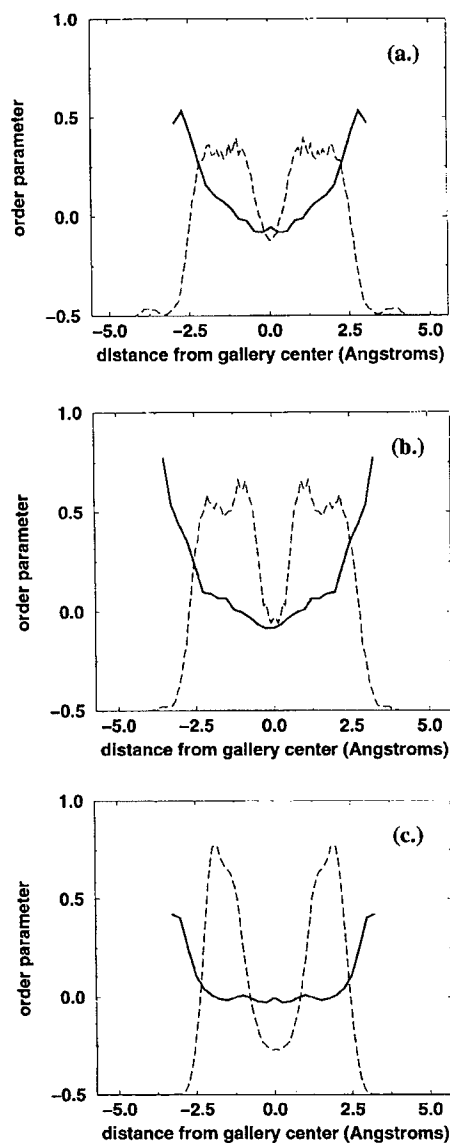


**Figure 5.** Order parameter of C-C-O bonds (solid lines) as a function of position in the silicate gallery. An order parameter of one implies that bonds lie flat against the surface, while random bond angle orientation results in an order parameter of approximately zero. The PEO (carbon and oxygen) density profiles (dashed lines) are shown for comparison. (a) Dry  $\text{Na}^+$ -montmorillonite/PEO nanocomposite; (b) dry  $\text{Li}^+$ -montmorillonite/PEO nanocomposite; (c) hydrated  $\text{Li}^+$ -montmorillonite/PEO nanocomposite.

For  $\theta = 0^\circ$ , corresponding to C-C-O bonds on planes flat against the surface, the order parameter will be equal to 1. For  $\theta = 90^\circ$ , meaning that a C-C-O bond lies normal to the surface, the order parameter is  $-0.5$ . These limiting cases are illustrated in Figure 4. An order parameter of approximately zero indicates random bond orientation.

Figure 5 shows the order parameter as a function of the bond position inside the gallery for the nanocomposites studied here. The bonds with a center of mass nearest the silicate surface have an order parameter of 0.5 or higher, indicating that these bonds are inclined to lie flat against the surface. Such surface-induced, or epitaxial, orientations next to the confining wall is expected. In the dry systems, which have more atomic-

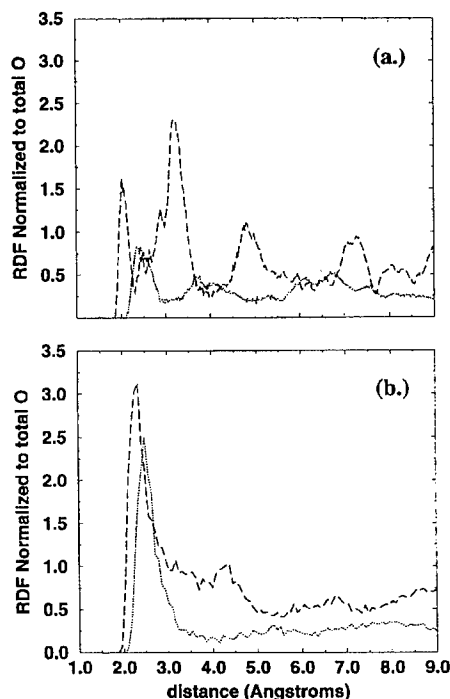


**Figure 6.** Radial pair correlation functions of cations and oxygen for the dry PEO nanocomposites: (a)  $\text{Na}^+$ -montmorillonite; (b)  $\text{Li}^+$ -montmorillonite. For both graphs: dashed line, PCF with silicate surface oxygens; dotted line, PCF with PEO oxygens.

level ordering, as seen in the finer details of their oxygen and carbon density profiles compared to those of the hydrated system, this ordering of the bonds extends a few Angstroms—less than a single atomic layer—further into the gallery. However, for the hydrated systems, this bond orientation does not extend any significant distance into the gallery. The bonds that are not directly on the silicate surface do not show any preferred orientation. The calculated average order parameter of C-C-O bonds for the whole PEO intercalated film is 0.06 for the dry and 0.03 for the hydrated  $\text{Li}^+$ -montmorillonite, respectively, showing a nearly random distribution of C-C-O bonds with respect to the silicate surface in both cases. It is likely that the bonds are unable to maintain a vertical orientation, as the spacing may suggest, because of the frequent obstacles caused by cations and water molecules. Also, the layer distribution of oxygen, as indicated by the density profiles, cannot be achieved with a strictly horizontal or vertical bond angle orientation of the ethylene oxide repeat unit. The additional layering, and to a lesser extent, ordering, of the oxygen in the dry  $\text{Na}^+$  or  $\text{Li}^+$ /PEO intercalated system is most likely due to the oxygen's effort to coordinate to the cations, rather than the confinement-induced ordering of the chain conformations. This feature disappears with the introduction of water, which replaces PEO oxygen in the cation coordination shells. In the water-containing systems, the polymer coordinates less to the cation, and thus it can more freely organize into a more pronounced bilayer, which is the configuration dictated by the steric constraint.

Radial pair correlation functions (PCF), shown in Figures 6 and 7, illustrate the degree of association between the cations and the various species containing oxygen in the system. The area under the first peak in

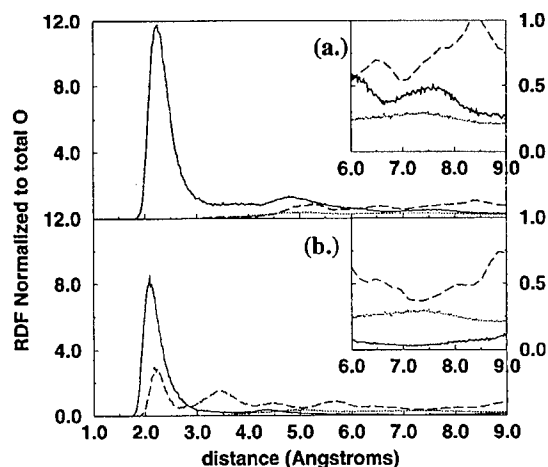


**Figure 7.** Pair correlation functions of  $\text{Li}^+$  ions and oxygen for the hydrated  $\text{Li}^+$ -montmorillonite/PEO nanocomposites. Insets show convergence at long distances. (a) Gallery center  $\text{Li}^+$ ; (b) silicate surface  $\text{Li}^+$ . Solid line, PCF with water oxygen atoms; heavy dashed line, PCF with silicate surface oxygens; light dotted line of both graphs, PCF between all  $\text{Li}^+$  and PEO oxygens.

the PCF represents the coordination between the cation and the type of oxygen being considered. In this two-dimensional system, PCFs cannot be assumed to provide the accurate topological information about the cations' coordination. However, whereas the density profiles average the structure throughout a given plane parallel to the silicate, the PCFs provide information pertinent to the ions' immediate surroundings. Taken together, the PCFs and density profiles complement each other to provide a complete statistical picture of the local structure of the nanocomposite. Inspection of the PCFs for the dry  $\text{Li}^+$ - and  $\text{Na}^+$ -montmorillonite systems show that these ions are coordinated by the PEO oxygen and, to a lesser extent, the silicate surface oxygen atoms (Figure 6). Coordination numbers are calculated by integrating the PCF to the "first minimum" and normalizing to the average density of the type of oxygen atom being considered. For consistency, the "first minima" were chosen by inspection as the point where the PCF curves appear to flatten out. Coordination numbers calculated in this way may not give ideal statistical values, but our intent is to show which species are dominant in coordinating the cations under different conditions. Coordination numbers calculated from the PCFs are given in Table 1. The PCF for  $\text{Na}^+$  and the silicate surface oxygen also shows a sharp second peak and several smaller oscillations at larger distances. This is due to the periodicity of the silicate crystal structure, so that the second peak corresponds to the next nearest neighbor in the surface oxygen structure, and so forth. Because the PCF represents an average over many different configurations, accounting for many likely positions of the ion as it vibrates or diffuses, the peaks become rounded or smeared out. This "smearing out" becomes more evident with distance. At a large distance, even the PCF between an ion and the highly periodic silicate structure will converge to 1, when the PCF is normalized to the average bulk density of the silicate surface oxygen. A more mobile atom, which samples more possible positions, will also lead to more "smearing out" of these secondary or higher order peaks. The

**Table 1. Cation-Oxygen Coordination Based on Integration of Pair Correlation Functions<sup>a</sup>**

species	number	PEO	surface O	total
$\text{Na}^+$ (dry system)	24	5.1 (2.9 Å)	1.2 (2.4 Å)	6.3
$\text{Li}^+$ (dry system)	24	2.3 (3.5 Å)	2.0 (2.7 Å)	4.2

species	number	$\text{H}_2\text{O}$	surface O	total
$\text{Li}^+$ (surface)	12	4.4 (3.0 Å)	1.2 (2.6 Å)	5.6
$\text{Li}^+$ (gallery center)	10	7.9 (3.0 Å)	0.02 (2.6 Å)	7.7
$\text{Li}^+$ (overall)	24	5.5 (3.0 Å)	1.1 (2.6 Å)	6.6

<sup>a</sup> Numbers in parentheses refer to the upper limit of integration of the PCFs in the calculation of these coordination numbers and correspond to the first minima of the PCFs. For the hydrated system, the number of overall  $\text{Li}^+$  ions is greater than the sum of surface and gallery center ions because it includes ions that jumped between the surface and gallery center during the course of the simulation, and thus were not included in either the surface or the central  $\text{Li}$ .

**Table 2. Self-diffusion Coefficients of Li and Water in the Li-Montmorillonite/PEO Nanocomposite Based on 1-ns Molecular Dynamics Simulation**

species	number	$D$ ( $\text{cm}^2/\text{s}$ )
$\text{Li}^+$ (surface)	12	$0.89 \times 10^{-8}$
$\text{Li}^+$ (gallery center)	10	$2.0 \times 10^{-8}$
$\text{Li}^+$ (overall)	24	$1.4 \times 10^{-8}$
$\text{H}_2\text{O}$	133	$8.0 \times 10^{-8}$

smaller size of the  $\text{Li}^+$  ion makes it more mobile than  $\text{Na}^+$ , even within the cavity of the silicate surface. Because of this, the PCF between the  $\text{Li}^+$  and the silicate surface oxygen is "smeared out" and begins to converge, even after the first peak.

The PCFs for the hydrated  $\text{Li}^+$ -montmorillonite system are shown in Figure 7. They show clearly that the  $\text{Li}^+$  is primarily coordinated by the water oxygen atoms. Because PCFs show the PEO oxygen atoms to be clearly outside of the  $\text{Li}^+$  coordination shell, they do not contribute to the calculation of the coordination numbers in the water-containing system. Table 1 shows the average number of oxygen atoms from the surface, PEO (for the dry system), and water (for the hydrated system) within the ions' primary coordination shells. All ions are considered together in each dry system. In the hydrated system, however, the ions in the gallery center are surrounded by water molecules, while oxygens from the silicate surface make up only a fraction of the coordination shell for the ions. In the absence of any external electric field, very few atoms move between a surface layer and the gallery center over the simulated time scale, so comparisons between surface ions and ions in the middle of the gallery are based on the ions that are clearly categorized as one type or the other throughout the simulation.

Table 2 shows the self-diffusion coefficients for water and  $\text{Li}^+$  based on mean-squared displacement during the course of the 1-ns simulation.  $\text{Li}^+$  cations in the middle of the gallery move faster than the cations near the silicate surface. This behavior reflects the ability of the surface to "trap" the  $\text{Li}^+$  cations in the crystal lattice cavities or above negatively charged substitutional sites in the octahedral layer of the silicate. It should be noted, however, that the time scale of the simulation was not sufficient to statistically study the movement of ions from one surface cavity to another. The steric limitations of the rigid, stationary surface and the polarization of neighboring water molecules also impede the  $\text{Li}^+$  mobil-

ity. At the surface, because there are relatively few water molecules in the hydration shell, the hydrating water molecules are more highly polarized and therefore more tightly attracted to the surface. Similarly, in studies of hydrated  $\text{Li}^+$ -montmorillonite, Sposito and co-workers have observed that surface complexes persisted while ions further from the surfaces formed a more mobile "diffuse layer" in two- and three-layer hydrates.<sup>10</sup>

When considering the mechanism of ionic motion, one may wonder whether the mobile ions drag their hydration shells with them or whether they move independently, exchanging one coordinating oxygen for another as they move. Water moves much faster than the  $\text{Li}^+$  throughout the gallery. That water is moving so much faster than the  $\text{Li}^+$  suggests that the local coordination environment of a  $\text{Li}^+$  ion is rapidly changing as the coordinating water molecules move on, and new ones move into their place or as the water molecules fluctuate in their distance from the ion which they coordinate. This rapidly changing environment may facilitate the ion's motion because the ion may find itself momentarily lacking a coordinating oxygen and may easily move toward the vacated space, effectively taking advantage of the water dynamics.

To compare the rate of change of coordination environment to ion mobility, we looked at how often a  $\text{Li}^+$  ion gained or lost a coordinating water molecule and compared ions near the surface to those in the center of the gallery. Molecules gained should equal molecules lost at equilibrium, and this is the case in our simulations. No attempt is made here to exclude molecules that leave and immediately return to the same hydration shell. In such a case, the ion would still have a chance to move into the free space while its neighbor was temporarily away. (In the case of conduction under an electric field, ions may be more likely to exchange neighbors because they, unlike water molecules, would migrate in a preferred direction.) For the gallery center, most ions exhibited over 300 losses or gains. More than  $2/3$  of ions with fewer observed losses and gains—on the order of 50—belonged to the layers near the surface. On one hand, although surface ions may have statistically few water molecules, stationary surface atoms make up the remainder of their coordination shells, and therefore

the surface ions have a less rapidly evolving coordination environment than ions in the middle of the gallery. On the other hand, the more mobile  $\text{Li}^+$  cations in the middle of the gallery have a more rapidly evolving coordination environment.

#### IV. Conclusions

Using computer simulations, we have shown that the intercalated polymer chains in a PEO-layered silicate nanocomposite are arranged in discrete subnanometer layers parallel to the crystalline silicate layers. Despite this ordering, the chains retain a disordered, liquid-like structure with no crystallinity or preferential ordering of the C—C—O bonds. This structure is in contrast to previously suggested configurations for intercalated PEO, but agrees well with more recent SANS experiments.

In the dry nanocomposites the cations reside primarily next to the silicate surface rather than being coordinated with PEO. In the hydrated nanocomposites, more than half of the cations present in the galleries exist in the layers near the silicate surfaces, partly inserted in the silicate surface cavities, and a few ions even appear to be translationally inhibited when burrowed within these crystalline cavities. Ions near the silicate surface move significantly more slowly than those in the center of the gallery. Water molecules, in general, diffuse more quickly than the ions.

Cations are primarily coordinated by water oxygen atoms, and to a lesser extent, by the silicate surface. In a hydrated system, the PEO oxygen atoms do not enter significantly into the cations' coordination cell. The ions' hydration environment changes most rapidly in the center of the gallery, where ion motion is faster. Because the changing coordination environment is related to the possibility the ions have for motion, the evolving hydration environment is related to the mobility of the ions.

**Acknowledgment.** This work was supported by the AFOSR. E.H. acknowledges an NSF Graduate Research Fellowship. We would like to acknowledge Dr. Juraj Bujdak for experimental data and useful discussions.

CM990676X